Available online at www.sciencedirect.com

SciVerse ScienceDirect

Ceramics International 38 (2012) 2369–2373

CERAMICS INTERNATIONAL

www.elsevier.com/locate/ceramint

Crystallization kinetics of Nd-substituted yttrium iron garnet prepared through sol–gel auto-combustion method

T. Arun, M. Vairavel, S. Gokul Raj[1], R. Justin Joseyphus*

Department of Physics, National Institute of Technology, Tiruchirappalli 620015, India

Received 22 October 2011; received in revised form 29 October 2011; accepted 31 October 2011
Available online 17 November 2011

Abstract

Nd substituted $Y_3Fe_5O_{12}$ (YIG) was synthesized using sol–gel auto-combustion method. The phases present in the samples were identified using XRD. The asprepared dried gel was found to transform to the rare earth iron garnet phase at lower temperature when the Nd concentration is lower. Higher concentration of Nd resulted in the formation of orthoferrite as the major phase. The Curie temperature was recorded using thermomagnetic analysis and it was found to increase with the concentration of Nd. The crystallization kinetics of the Nd-substituted garnet phase was studied using TG–DTA. Two stage crystallization was observed from the DTA analysis for $Nd_1Y_2Fe_5O_{12}$. The activation energy for the formation of $Nd_1Y_2Fe_5O_{12}$ was 610 kJ/mol, found by using Johnson–Mehl–Avrami (JMA) equation. Three dimensional growth mechanism dominate at lower heating rates for the Nd-substituted YIG.

Keywords: A. Sol–gel processes; C. Thermal properties; Johnson–Mehl–Avrami model

1. Introduction

Rare earth iron garnets (RIGs) are used in magneto-optical and microwave applications [1–3]. The rare earth iron garnets have the general formula $R_3Fe_5O_{12}$ where R can be a rare earth ion such as Y, Gd, Nd or a combination of these ions. The magnetic properties of RIG depend on the site occupancy of the rare earth and iron ions among the various cation sites in the cubic crystal structure [4]. The cation sites in RIG can be classified as dodecahedral {c} site which is occupied by rare earth ion and octahedral [a], tetrahedral (d) sites which are occupied by Fe ions. The {c} sublattice magnetization is equal and opposite to the resultant of the [a] and (d) sublattice magnetizations at the compensation temperature. At the Curie temperature, all the sublattice moments are randomly oriented and become paramagnetic. The synthesis conditions affect the crystallinity, which in turn alters the magnetic properties of RIG.

Various synthesis methods have been attempted by researchers to synthesize pure RIG. Unlike spinel ferrites which could be synthesized at temperatures below 573 K using chemical methods [5,6], the phase formation of RIG requires temperature above 1573 K [4,7]. Attempts were made to reduce the crystallization temperature in yttrium iron garnets (YIG) prepared using sol–gel [8], co-precipitation [9] and solid state reaction [10] methods. The knowledge of crystallization behavior shall be useful for the synthesis of RIG at reduced annealing temperatures. In this paper, we present the crystallization kinetics of Nd substituted yttrium iron garnet prepared using sol–gel autocombustion technique.

2. Experimental procedure

$Nd_xY_{3-x}Fe_5O_{12}$ ($x = 1.0, 1.5, 2.0$) was synthesized using the sol–gel autocombustion method. The starting precursors used in the synthesis are neodymium, yttrium and iron nitrates. The rare earth to iron nitrates were weighed in the ratio 3:5 and mixed with 50 ml double distilled water and used for further synthesis. Citric acid was added to the mixture with an oxide to fuel ratio 1, and mixed thoroughly to obtain a clear solution at room temperature. The stirring was continued along with heating in a beaker at 343 K for nearly 3 h to obtain a gel. The

---

* Corresponding author. Tel.: +91 431 250 3614.
E-mail address: rjustinj@nitt.edu (R. Justin Joseyphus).

[1] Present address: Vel. Tech. Dr. RR & Dr. SR Technical University, Avadi, Chennai 600062, India.

0272-8842/$36.00 © 2011 Elsevier Ltd and Techna Group S.r.l. All rights reserved.
doi:10.1016/j.ceramint.2011.10.090

obtained gel was rapidly heated at 573 K and upon igniting a solid precursor was obtained within 10 min which was used for further studies.

The phase analysis was carried out in a Rigaku X-ray Diffractometer (XRD) using Cu K_α. Thermal analysis was performed using EXSTAR 6200 Thermogravimetric analyzer/ Differential Thermal Analyzer (TG/DTA) at temperatures up to 1273 K. Thermomagnetic analysis was performed using the same equipment where the sample is subject to a magnetic field using a permanent magnet. The peak analysis and fittings were carried out using Origin 8 software.

3. Results and discussion

Fig. 1 shows the TG plot at a heating rate of 20 K/min for the asprepared $Nd_xY_{3-x}Fe_5O_{12}$ synthesized using the sol–gel autocombustion method with (a) $x = 0$ and (b) $x = 1$. Weight losses are observed at 373 and 670 K corresponding to the loss of water and removal of organic residues, respectively for both $x = 0$ and 1. The weight loss in the temperature range 1037–1070 K indicates the transformation of the complex to the oxide.

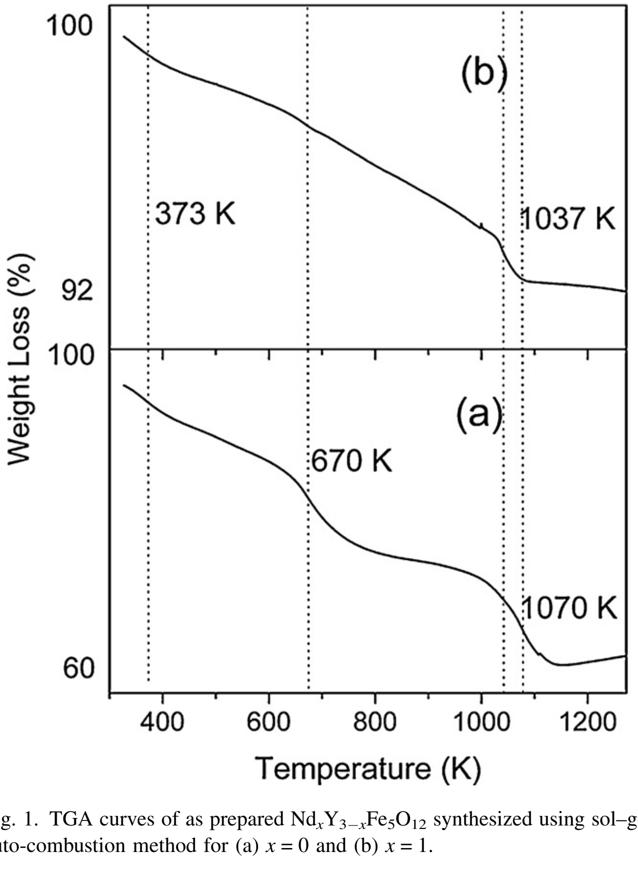

Fig. 1. TGA curves of as prepared $Nd_xY_{3-x}Fe_5O_{12}$ synthesized using sol–gel auto-combustion method for (a) $x = 0$ and (b) $x = 1$.

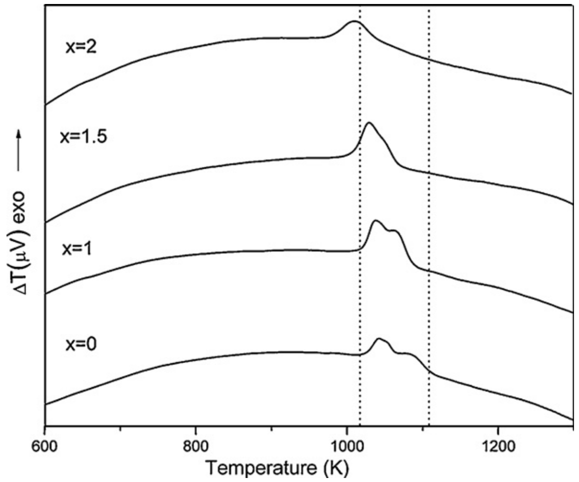

Fig. 2. Differential Thermal Analysis (DTA) curves of $Nd_xY_{3-x}Fe_5O_{12}$ synthesized using sol–gel auto-combustion method for $x = 0$, 1.0, 1.5 and 2.0.

Fig. 2 shows the DTA curves at a heating rate of 20 K/min for the asprepared $Nd_xY_{3-x}Fe_5O_{12}$ ($x = 0$, 1.0, 1.5, 2.0) synthesized using the sol–gel auto combustion method. Two exothermic peaks are observed in the temperature range 1040–1065 K for $x = 0$. The exothermic peaks indicate the crystallization of the RIG phase in two stages. These peaks are shifted towards the low temperature region with increasing x and only a single peak is observed at 1010 K for $x = 2$. This suggests a single stage crystallization event. However, in order to verify the formation of RIG phase, the samples were annealed at 1123 K. The XRD pattern of $Nd_xY_{3-x}Fe_5O_{12}$ ($x = 0$, 1.0, 1.5, 2.0) annealed at 1123 K is shown in Fig. 3. The garnet phase is observed predominantly in the case of $x = 0$ and 1 whereas orthoferrite ($RFeO_3$) phase is dominant for $x = 1.5$ and 2.0 along with other oxide phases. This suggests that the higher concentration of Nd prevents the crystallization of the garnet phase. Hence the presence of double peak in DTA for $x = 0$ and 1 may be due to the crystallization of orthoferrite followed by the formation of RIG phase at higher temperature. However at Nd concentrations larger than $x = 1.5$, the RIG phase is

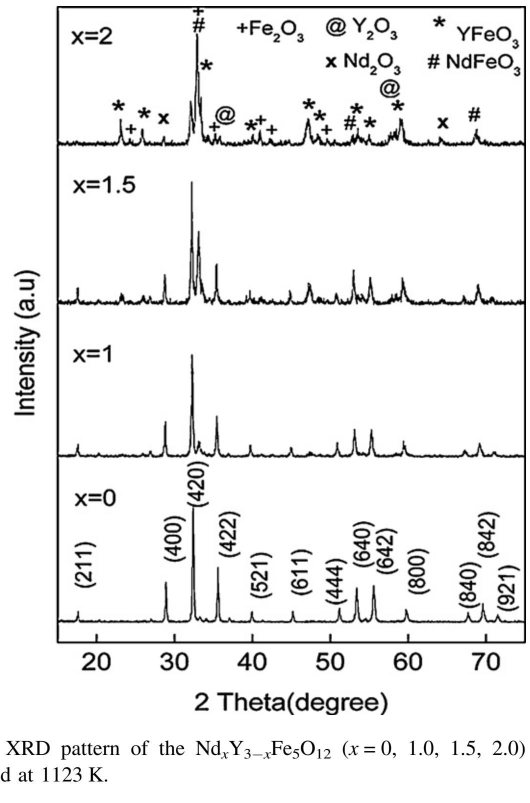

Fig. 3. XRD pattern of the $Nd_xY_{3-x}Fe_5O_{12}$ ($x = 0$, 1.0, 1.5, 2.0) samples annealed at 1123 K.

suppressed. The average grain size of the YIG is 40 nm whereas it decreases to 32 nm when substituted with Nd ($x = 1$). The above results suggest that the oxide to fuel ratio may be optimum only for the formation of YIG. The lattice parameter increases from 12.36 to 12.40 Å for $x = 0$ and 1, respectively, which indicate the incorporation of Nd into the lattice of YIG. It is difficult to estimate the average grain size and lattice parameter for the other samples due to overlapping peaks.

The thermomagnetic weight loss for the $Nd_xY_{3-x}Fe_5O_{12}$ ($x = 0$, 1.0, 1.5, 2.0) samples heated at 1123 K were recorded in the presence of an applied magnetic field. The weight loss indicates the Curie temperature (T_c) of the samples. The presence of $RFeO_3$ shall not affect the T_c due to its non magnetic nature. Fig. 4 shows the Curie temperature of the $Nd_xY_{3-x}Fe_5O_{12}$ with various Nd concentrations ($x = 0$, 1.0, 1.5, 2.0). The systematic increase in T_c from 527 to 560 K with increasing Nd could be observed. The T_c of bulk YIG is 550–560 K whereas the measurement of the same in TG is influenced by parameters such as magnetization of the sample, heating rate and applied field. Thus the T_c is shifted by nearly 25 K for all the samples. The T_c is influenced by the type of magnetic ions in the various sublattices. Consequently a variation from 587 K to 64 K has been observed depending on the type of substituent [4]. From our present studies an increase in T_c by 33 K is observed for Nd substitution up to $x = 2$.

In order to study the crystallization behavior of Nd-doped YIG, the activation energy for crystallization was evaluated for $Nd_1Y_2Fe_5O_{12}$. It should be noted that Nd concentration above 1 resulted in higher fraction of $RFeO_3$ and hence not suitable for the study. The activation energy for crystallization was determined by the phenomenological Johnson–Mehl–Avrami (JMA) equation [11–13].

The amount of crystallization at time t is given by the equation:

$$X(t) = 1 - \exp[-(Kt)^n] \tag{1}$$

where n is the Avrami exponent (dimensionless parameter related to the reaction mechanism) and K is the reaction rate constant in s^{-1}.

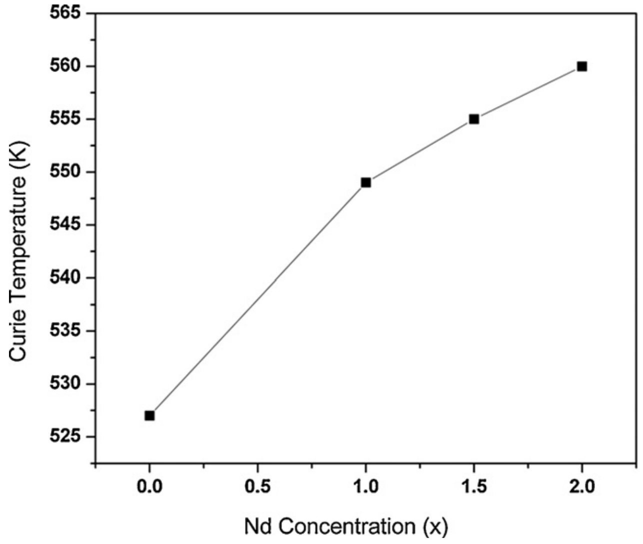

Fig. 4. The Curie temperature of $Nd_xY_{3-x}Fe_5O_{12}$ found from thermomagnetic analysis for various values of x.

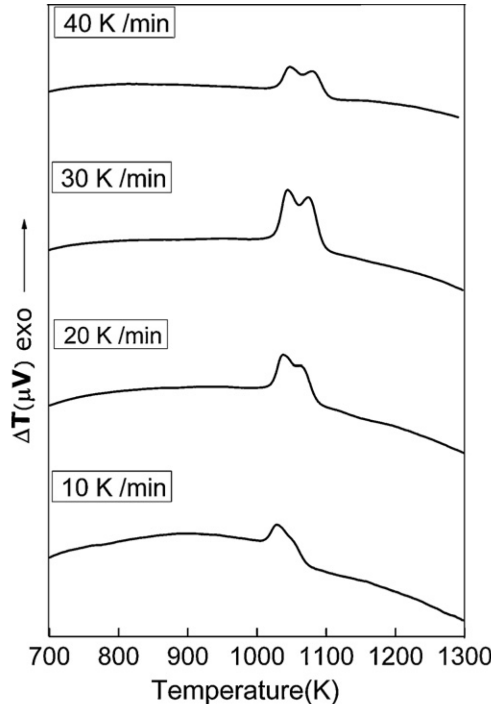

Fig. 5. DTA curves of $Nd_1Y_2Fe_5O_{12}$ gel heated at 10, 20, 30 and 40 K/min.

The reaction rate constant is obtained from Arrhenius equation:

$$K = V\exp\left(\frac{-E_a}{RT}\right) \tag{2}$$

where E_a is the Activation energy for crystallization in kJ/mol, T is the absolute temperature in K and V is the frequency factor in s^{-1}.

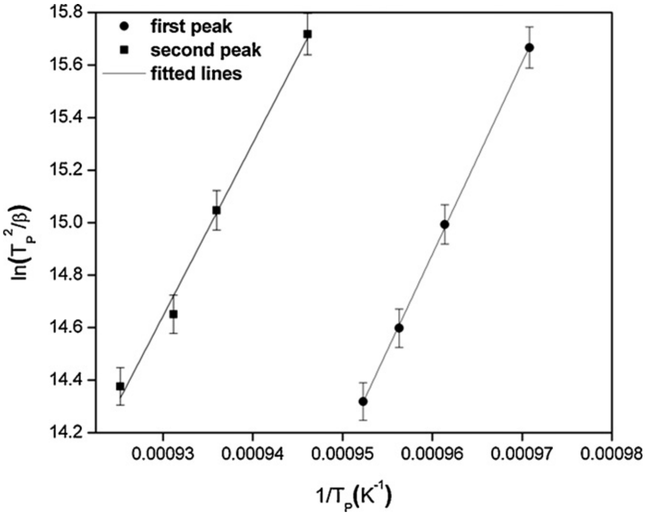

Fig. 6. JMA plot for $Nd_1Y_2Fe_5O_{12}$ corresponding to the two crystallization peaks found from DTA.

Table 1
The Avarami exponent (n) values of $Nd_1Y_2Fe_5O_{12}$ for the two crystallization peaks observed from the DTA.

Peak	Heating rate (K/min)	ΔT (K)	T (K)	E_a/R (K)	n	Reaction mechanism
1	10	43.31	1030	73068.7	0.8	
1	20	31.33	1040	73068.7	1.2	Surface nucleation
1	30	20.89	1045	73068.7	1.8	
1	40	27.72	1050	73068.7	1.4	
2	10	11.75	1056	65750.2	3.6	Three-dimensional growth
2	20	17.31	1068	65750.2	2.5	
2	30	18.83	1073	65750.2	2.3	One/two dimensional growth
2	40	17.03	1080	65750.2	2.6	

From these equations, the JMA equation was derived given by Eq. (3):

$$\ln\left(\frac{T_p{}^2}{\beta}\right) = \ln\left(\frac{E_a}{R}\right) - \ln V + \left(\frac{E_a}{RT}\right) \qquad (3)$$

where β is the heating rate in K/s, T_p is the crystallization peak temperature in K and R is the gas constant.

The activation energy of $Nd_1Y_2Fe_5O_{12}$ was calculated using the JMA equation from the DTA curves at various heating rates. The DTA curves of the asprepared $Nd_1Y_2Fe_5O_{12}$ gel heated at 10, 20, 30, and 40 K/min are shown in Fig. 5. At higher heating rates two exothermic peaks were observed in the DTA whereas they merge together at lower heating rate. The two peaks were fitted by Gaussian function to find the full width half maximum and the peak positions. It could be understood from the previous discussions that the first peak corresponds to $RFeO_3$ and the second one corresponding to the formation of the garnet phase. Fig. 6 shows the JMA plot for $Nd_1Y_2Fe_5O_{12}$. The activation energy for crystallization was found from the slope of the lines using Eq. (3). The activation energy for crystallization of $RFeO_3$ and $Nd_1Y_2Fe_5O_{12}$ were found as 546 kJ/mol and 610 kJ/mol, respectively. The activation energy for Bi substituted $Y_3Fe_5O_{12}$ prepared using coprecipitation method was found to show values ranging from 650 kJ/mol for $Bi_{0.75}$ [14] to 1023 kJ/mol for $Bi_{1.25}$ [15]. However the value of 610 kJ/mol for $Nd_1Y_2Fe_5O_{12}$ suggests that the activation energy is lower for rare earth ion substitution using the present synthesis method.

The Avrami exponent is a dimensionless factor relating with the reaction mechanism. The equation for n is given by [16]:

$$n = 2.5T_p^2 \frac{R}{\Delta T E_a} \qquad (4)$$

where $\triangle T$ is the full width at half maximum of the peak.

The n value indicates the reaction mechanism which ranges from surface nucleation for $n = 1$ to three dimensional growth for $n = 4$.

Table 1 shows the n values of $Nd_1Y_2Fe_5O_{12}$ obtained from the Avarami exponent. The average (n) value for the first crystallization peak ($RFeO_3$) is 1.3 whereas it is 2.8 for the second peak. From the table, it could be understood that surface nucleation dominates for the formation of $RFeO_3$ whereas it is two dimensional growth for the crystallization of $Nd_1Y_2Fe_5O_{12}$. Also, slow heating resulted in three dimensional growth corresponding to $n = 3.6$ for $Nd_1Y_2Fe_5O_{12}$.

4. Conclusion

$Y_3Fe_5O_{12}$ and Nd substituted $Y_3Fe_5O_{12}$ were synthesized using sol–gel auto-combustion method. Higher concentration of Nd resulted in the formation of orthoferrite as the major phase. The Curie temperature was found to increase with the substitution of Nd in $Y_3Fe_5O_{12}$. The activation energy for crystallization of $Nd_1Y_2Fe_5O_{12}$ was found to be 610 kJ/mol using Johnson–Mehl–Avrami (JMA) equation. Three dimensional growth mechanism dominates during the crystallization of $Nd_1Y_2Fe_5O_{12}$ at lower heating rates.

Acknowledgements

The authors acknowledge the DST, Govt. of India for the partial financial assistance through FAST track project (SR/FTP/ETA-11/2008) sanctioned to RJJ.

References

[1] P.M. Ollivier, Microwave YIG-tuned transistor oscillator amplifier design: application to C band, IEEE J. Solid-State Circ. SC-7 (1972) 54–60.

[2] K.H.J. Buschow, Magneto-optical recording materials, J. Less Common Met. 155 (1989) 307–318.

[3] W.R. Eppler, M.H. Kryder, Garnets for short wavelength magneto-optical recording, J. Phys. Chem. Solids 56 (1995) 1479–1490.

[4] G. Winkler, Magnetic Garnets, Friedr. Vieweg, Sohn, Braunschweig/Wiesbaden, 1981.

[5] S. Sun, H. Zeng, D.B. Robinson, S. Raoux, P.M. Rice, S.X. Wang, G. Li, Monodisperse MFe_2O_4 ((M) Fe, Co, Mn) nanoparticles, J. Am. Chem. Soc. 126 (2004) 273–279.

[6] R. Justin Joseyphus, A. Narayanasamy, K. Shinoda, B. Jeyadevan, K. Tohji, Synthesis and magnetic properties of the size-controlled Mn–Zn ferrite nanoparticles by oxidation method, J. Phys. Chem. Sol. 67 (2006) 1510–1517.

[7] X.Z. Guo, B.G. Ravi, P.S. Devi, J.C. Hanson, J. Margolies, R.J. Gambino, J.B. Parise, S. Sampath, Synthesis of yttrium iron garnet (YIG) by citrate–nitrate gel combustion and precursor plasma spray processes, J. Magn. Magn. Mater. 295 (2005) 145–154.

[8] M. Pal, D. Chakravorty, Synthesis of nanocrystalline yttrium iron garnet by sol–gel route, Physica E 5 (1999) 200–203.

[9] W. Zhang, C. Guo, R. Ji, C. Fang, Y. Zeng, Low-temperature synthesis and microstructure-property study of single-phase yttrium iron garnet (YIG)

nanocrystals via a rapid chemical coprecipitation, Mater. Chem. Phys. 125 (2011) 646–651.

[10] H. Yu, L. Zeng, C. Lu, W. Zhang, G. Xu, Synthesis of nanocrystalline yttrium iron garnet by low temperature solid state reaction, Mater. Charact. 62 (2011) 378–381.

[11] D.W. Henderson, Experimental analysis of non-isothermal transformations involving nucleation and growth, J. Therm. Anal. 15 (1979) 325–331.

[12] D.W. Henderson, Thermal analysis of non-isothermal crystallization kinetics in glass forming liquids, J. Non-Cryst. Solids 30 (1979) 301–315.

[13] P. Shepilovm, D.S. Baik, Computer simulation of crystallization kinetics for the model with simultaneous nucleation of randomly-oriented ellipsoidal crystals, J. Non-Cryst. Solids 171 (1994) 141–156.

[14] Y.P. Fu, D.S. Hung, C.W. Cheng, F.Y. Tsai, Y.D. Yao, Non-isothermal crystallization kinetics and microwave properties of $Bi_{0.75}Y_{2.25}Fe_5O_{12}$ prepared by coprecipitation, Ceram. Int. 35 (2009) 559–564.

[15] Y.P. Fu, K.K. Lew, Crystallization behavior of $Bi_{1.25}Y_{1.75}Fe_5O_{12}$ prepared by coprecipitation process, Ceram. Int. 35 (2009) 3235–3239.

[16] J.D. Menczel, R.B. Prime, Thermal Analysis of Polymers: Fundamentals and Applications, John Wiley and Sons, Inc., Hoboken, New Jersey, 2009